Supplementary Information

Tunable long-range spin transport in van der Waals $Fe_3GeTe_2/WSe_2/Fe_3GeTe_2$ spin valve

Anil Kumar Singh[a], Weibo Gao[b], and Pritam Deb[a]*
*Corresponding authors
[a] Advanced Functional Materials Laboratory, Department of Physics, Tezpur University (Central University), Tezpur 784028, India
*Email: pdeb@tezu.ernet.in
[b] Division of Physics and Applied Physics, School of Physical and Mathematical Sciences, Nanyang Technological University, Singapore 639798, Singapore

Crystal structure optimization provides details of charge and magnetic moments of each atom along-with absolute magnetization of the system. By employing optimization calculations, we observed that ML-WSe_2 is nonmagnetic, whereas ML-FGT possess ferromagnetic behaviour with total magnetization of 6.27 Bohr mag/unit cell. On the other hand, vdW system features large total magnetization of the order of 37.48 Bohr mag/cell in parallel spin configuration. However, experimental study has shown that the junction can be operated over wide range of bias with electrically stable structure. Fig. 1a represents space group P63/mmc exhibiting hexagonal crystal structure of single layer FGT with lattice parameters a =b3.99Å, $c = 16.33$Å $\wedge$ $\alpha = \beta = 90°, \gamma = 120°$. It consists of five atomic layers in which Fe_3Ge slab sandwiched between two layers of Te atoms. Fig. 1b disclose the presence of both itinerant states in the proximity of fermi level (E_F) and nearly flat bands away from E_F. Also, crossing of bands across fermi level in company with band splitting represents itinerant metallic FM nature. The sharp peaks away from fermi level and hump near to fermi level as observed from DOS as shown in fig. 1c confirms the concurrence of itinerant and localized states. It is also observed that spitting of bands due to asymmetry in spin up and spin down states strongly dependent on energy. Further, spin polarization calculation as shown in fig. 1d represents the strong energy dependency with spin up state dominant at fermi level. At the same time, it changes it sign from positive to negative along with magnitude with the change in energy.

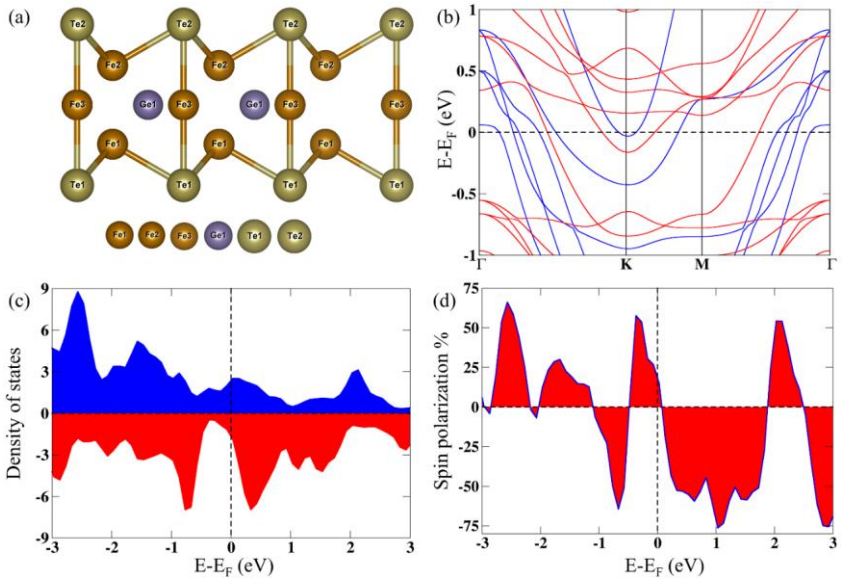

Fig. S1: Electronic properties of ML-Fe_3GeTe_2 (FGT). (a) atomic configuration (side-view), (b) band structure, (c) density of states (DOS) and (d) spin polarization %.

Furthermore, electronic structure calculations of ML-WSe_2 [Fig. S1] represent semiconducting nature with direct band gap at K- high symmetry point.

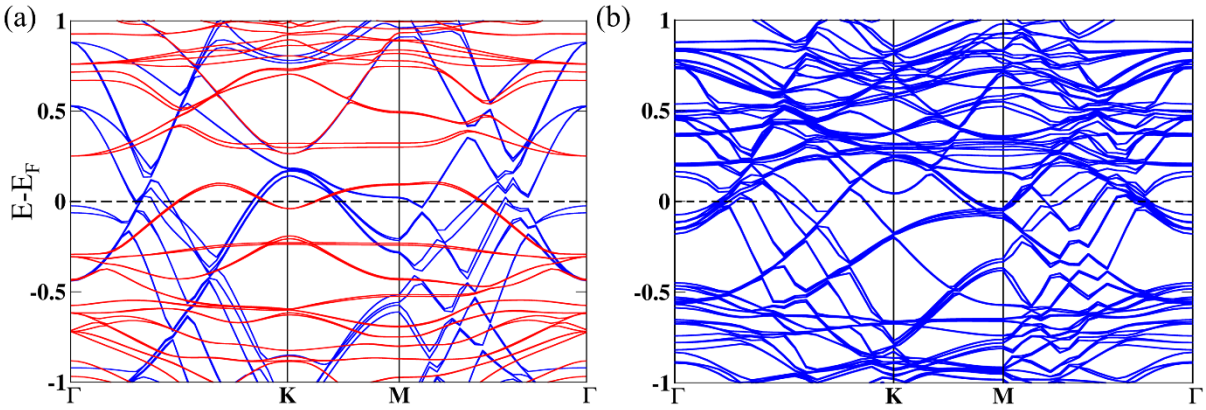

Fig. S2: represents band structures of FGT/WSe_2/FGT vdW heterostructure in presence of (a) DFT+U and (b) Spin-orbit coupling respectively.

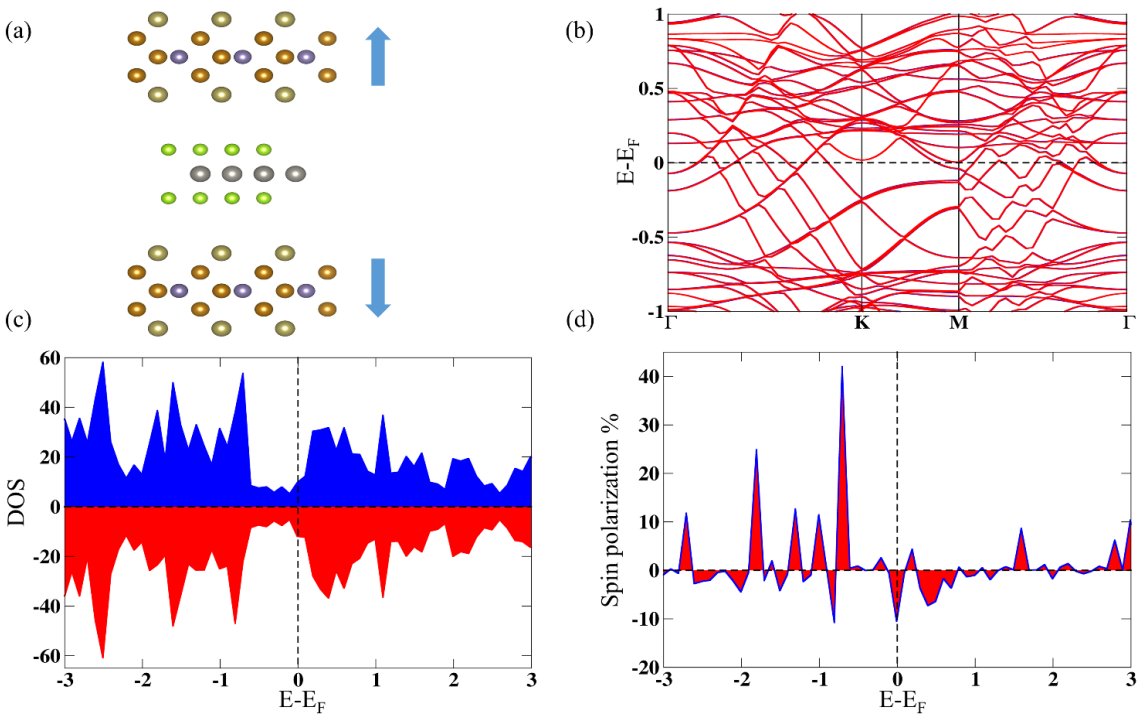

Fig. S3: Electronic properties of FGT-WSe_2-FGT vdW heterostructure system in antiparallel magnetization configuration. (a) side (top panel) and top view (bottom panel) of atomic configuration, (b-c) band structure and DOS respectively and (d) spin polarization %.

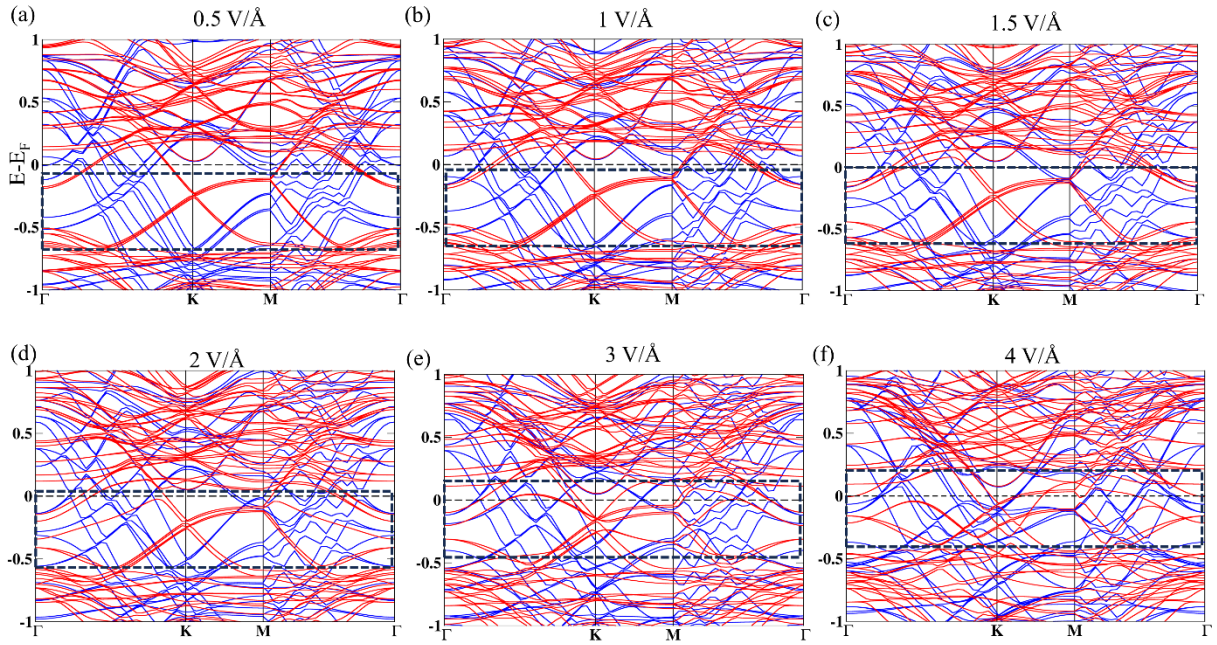

Fig. S4: Effect of electric field on band structure of vdW system in PC alignment. (a-f) represents band structure under electric field varying from 0.5 V/Å to 4 V/Å respectively.

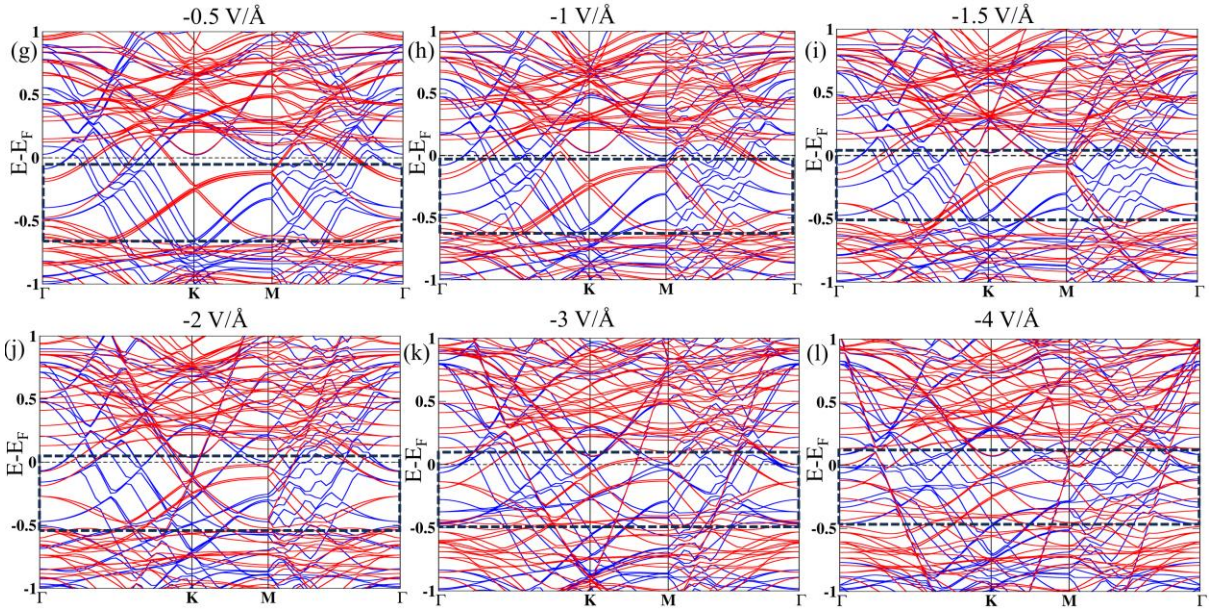

Fig. S5: Effect of electric field applied along -z direction on band structure of vdW system in PC alignment. (g-l) represents band structure under electric field varying from -0.5 V/Å to -4 V/Å respectively.

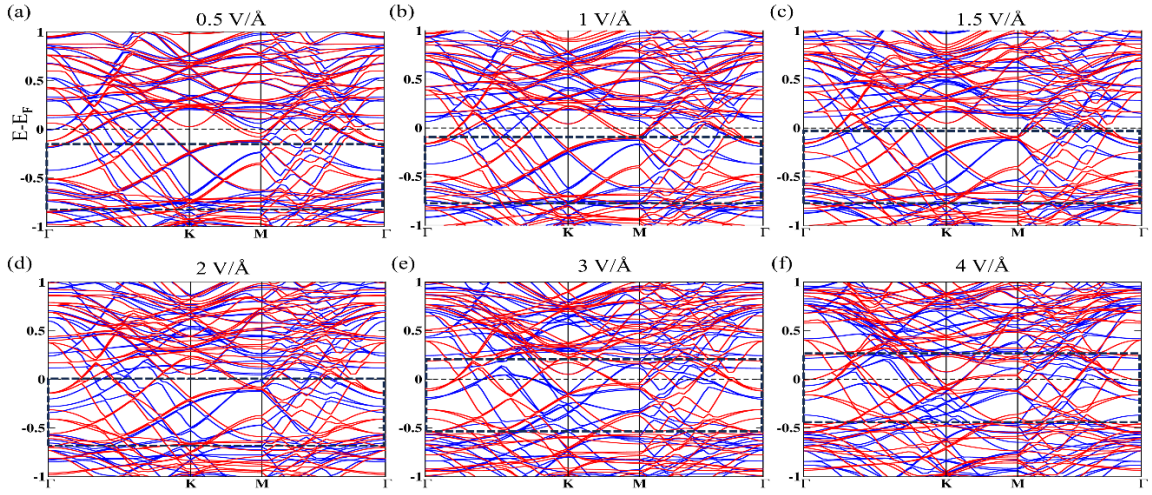

Fig. S6: Effect of electric field on band structure of vdW system in APC alignment. (a-g) represents band structure under electric field varying from 0.5 V/Å to 4 V/Å respectively.

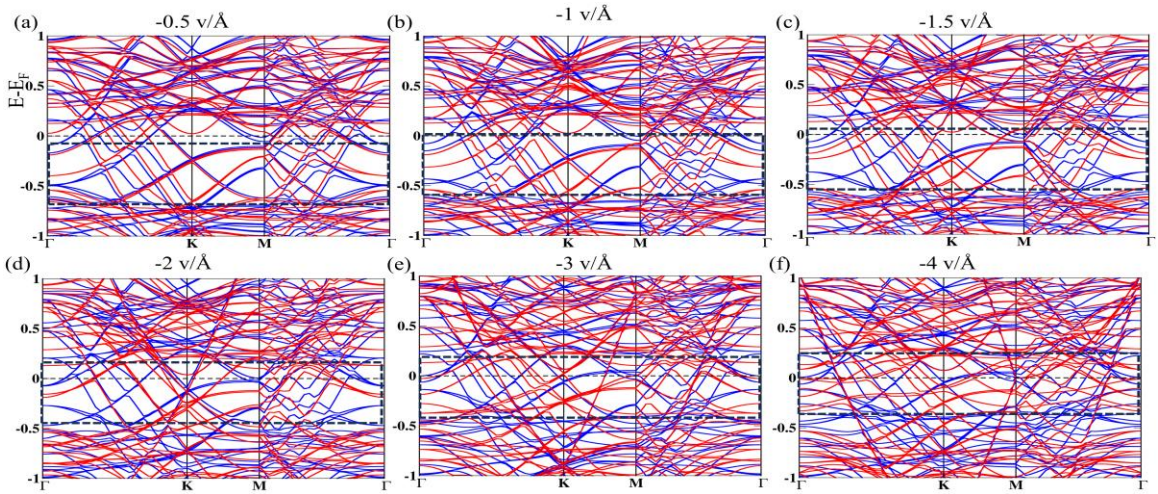

Fig. S7: Effect of electric field on band structure of vdW system in APC alignment. (a-f) represents band structure under electric field varying from -0.5 V/Å to -4 V/Å respectively.

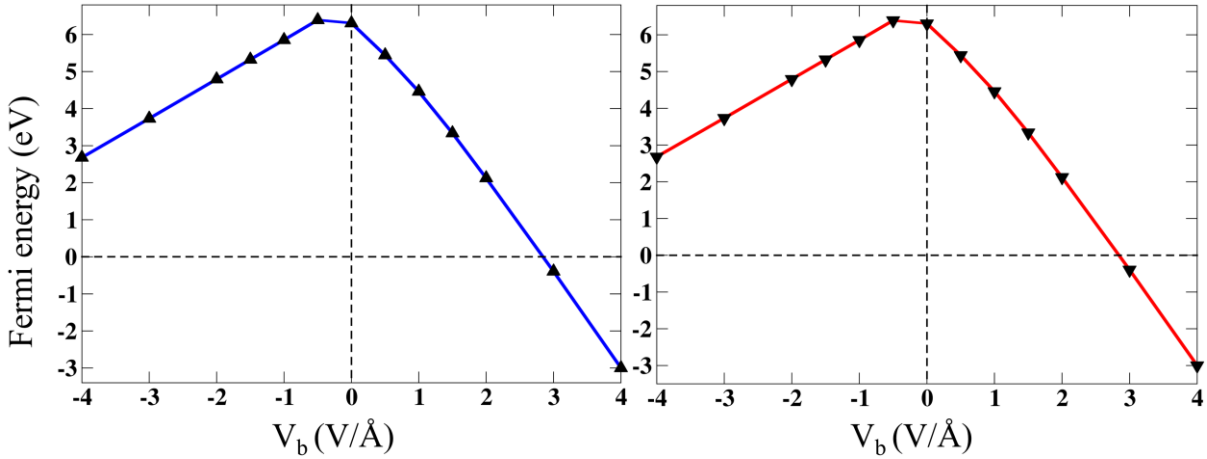

Fig. S8: Effect of electric field varying from -4 V/Å to 4 V/Å on Fermi energy of the vdW system in (a) parallel and (b) antiparallel configurations respectively.

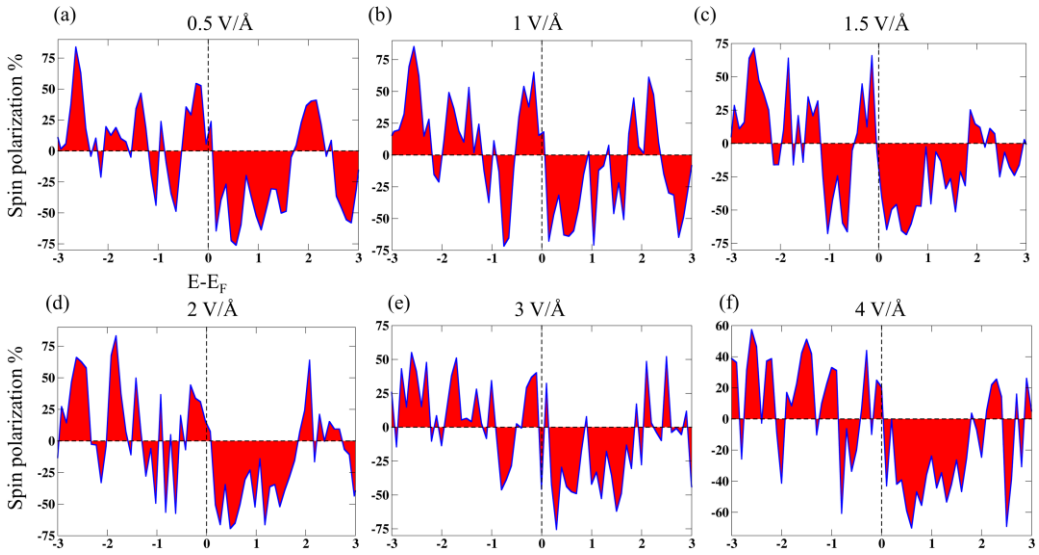

Fig. S9: Effect of electric field on spin polarization % of vdW system in PC alignment. (a-f) represents SP% under electric field varying from 0.5V/Å to 4V/Å respectively.

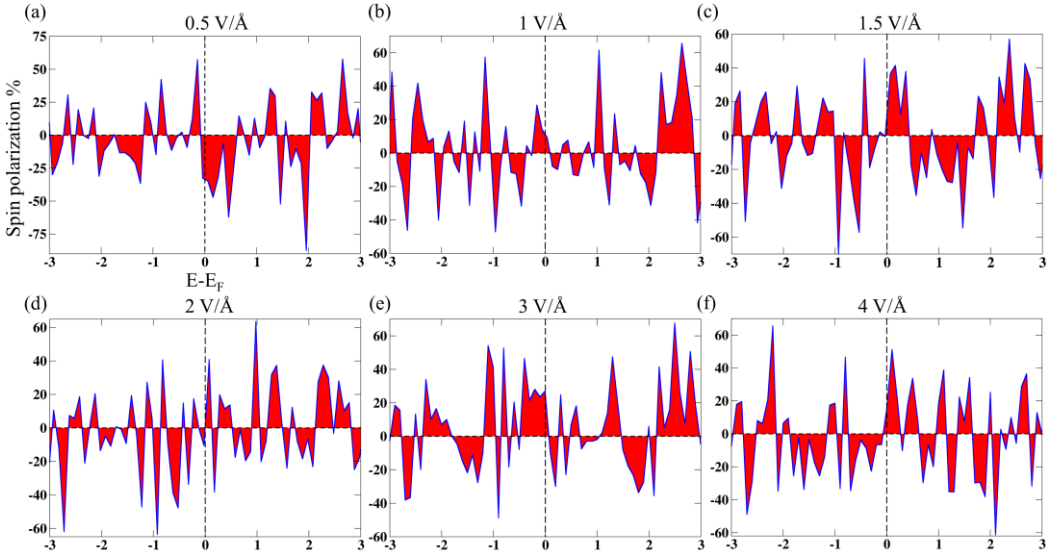

Fig. S10: Effect of electric field on spin polarization % of vdW system in APC alignment. (a-f) represents SP% under electric field varying from 0.5V/Å to 4V/Å respectively.

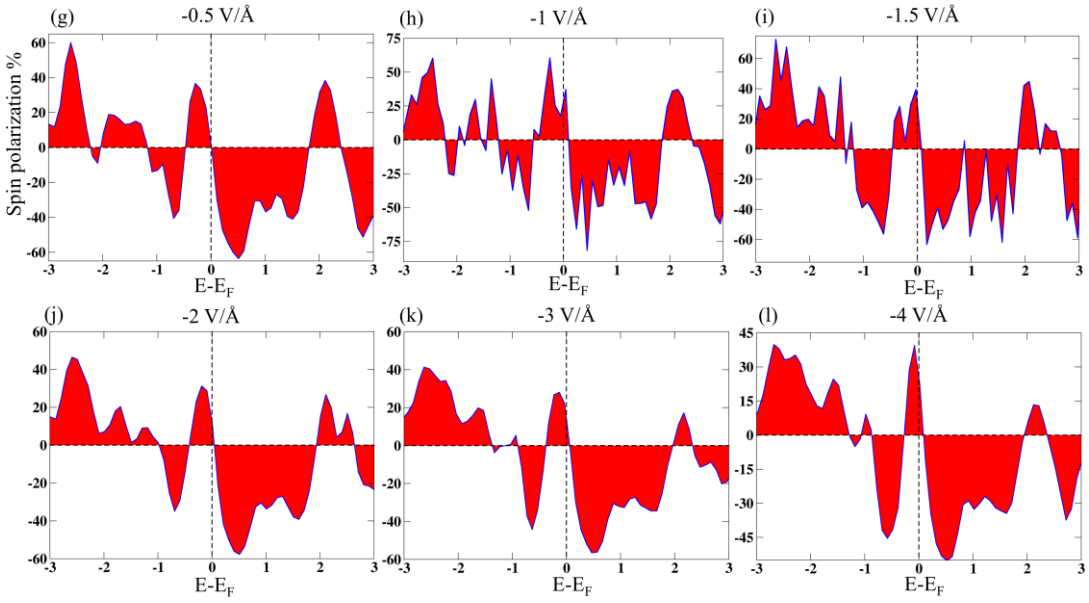

Fig. S11: Effect of electric field on spin polarization % of vdW system in PC alignment. (a-f) represents SP% under electric field varying from -0.5V/Å to -4V/Å respectively.

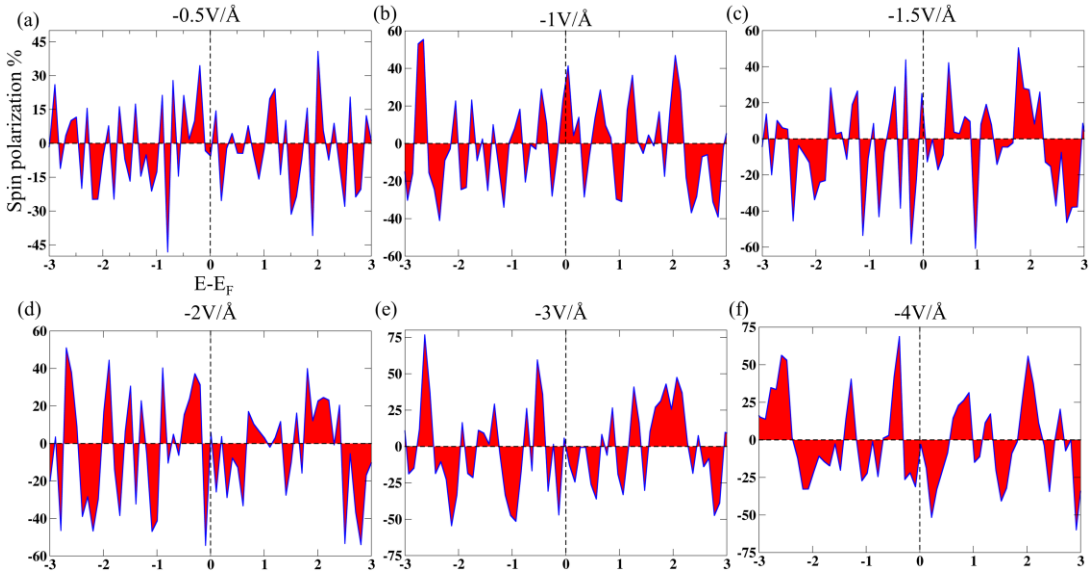

Fig. S12: Effect of electric field on spin polarization % of vdW system in APC alignment. (a-f) represents SP% under electric field varying from -0.5V/Å to -4V/Å respectively.

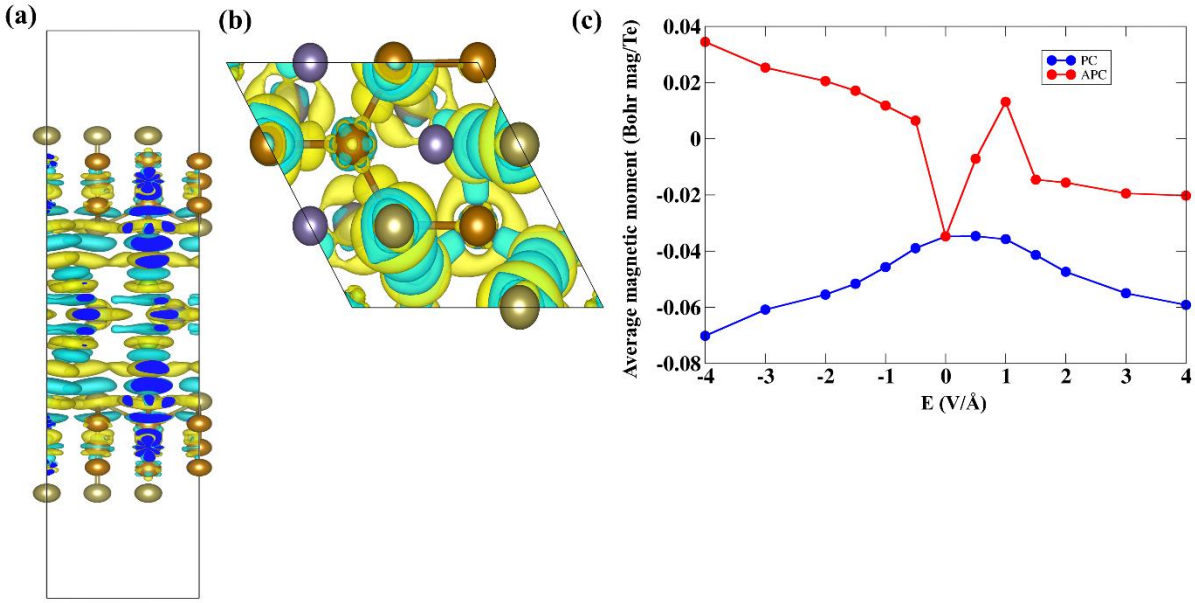

Fig. 13: Differential charge density (a) side view, (b) top view and (c) depicts variation in average magnetic moments of Te atoms. Here, yellow and cyan color corresponds to accumulation and depletion of charge at interface respectively.